

# The Superconducting Gap in MgB<sub>2</sub>: Electronic Raman Scattering Measurements of Single Crystals

J. W. Quilty, S. Lee, A. Yamamoto and S. Tajima

*Superconductivity Research Laboratory, International Superconductivity Technology Center,  
1-10-13 Shinonome, Koto-ku, Tokyo 135-0062, Japan*

We have performed polarisation-resolved Raman scattering measurements on MgB<sub>2</sub> single crystals to determine the magnitude, symmetry and temperature dependence of the superconducting gap. A single sharp peak due to Cooper pair breaking appears in the electronic continuum below  $T_c$ , reaching an average maximum Raman shift of  $105 \pm 1 \text{ cm}^{-1}$  ( $2\Delta(0)/k_B T_c = 3.96 \pm 0.09$ ) and showing up to  $5 \text{ cm}^{-1}$  anisotropy between polarised and depolarised spectra. The temperature dependence of  $2\Delta$  follows that predicted from BCS theory, while the anisotropy decreases with decreasing temperature. We conclude that our Raman results are consistent with a slightly anisotropic *s*-wave gap in a conventional BCS superconductor.

PACS numbers: 74.25.Gz, 74.70.Ad, 78.30.Er

The recently discovered superconductor MgB<sub>2</sub> shows an unusually high  $T_c$  for a simple binary compound, immediately raising the question of whether a conventional phonon-mediated pairing mechanism could be responsible for superconductivity [1–6]. Experiments on polycrystalline MgB<sub>2</sub> samples [7–11] report gap to  $T_c$  ratios from 0.6–4.2, spanning the range of regimes from sub-BCS to strong-coupling. Due to the difficulties and uncertainties associated with polycrystal measurements, these results strongly motivate further study of the gap feature(s) in single crystals.

Electronic Raman scattering is a useful experimental technique for studying superconductors because it provides a direct probe of the superconducting gap via the breaking of Cooper pairs by the incident light [12]. The position, polarisation dependence and temperature dependence of the pair breaking peak reflect the magnitude, symmetry and temperature dependence of the gap [12–14]. Knowledge of these fundamental properties is essential for the underlying mechanism of superconductivity to be deduced. In this letter we report the first Raman measurements of these gap properties in single crystals of MgB<sub>2</sub>.

Single crystals of MgB<sub>2</sub> were synthesized from a precursor mixture of 99.9% pure magnesium powder and 97% pure amorphous boron. The crystals were grown in a BN container under 4–6 GPa pressure at 1400–1700°C for 5 to 60 minutes. Magnetization and resistivity measurements of the superconducting transition give  $T_c = 38.2 \pm 0.3 \text{ K}$  [15]. Crystals with relatively clean and flat surfaces were selected for Raman scattering measurements; these crystals were roughly square in shape and of typical size 200–300  $\mu\text{m}$ .

Raman spectra were measured with a Jobin-Yvon T64000 triple monochromator, charge coupled device, and an excitation wavelength of 514.5 nm and typical power 0.8 mW provided by an Ar-Kr laser. The inci-

dent light was polarised either vertically (V) or horizontally (H) and point-focussed to a spot of 100  $\mu\text{m}$  diameter; only vertically polarised scattered light was collected. Henceforth we refer to the VV and HV configurations as *polarised* and *depolarised*. Single crystals were mounted on the cold finger of a closed-cycle helium refrigerator and at typical laser powers sample overheating was estimated to be less than 2 K, while spectra taken at higher powers showed evidence of up to 12 K overheating. Where appropriate, we have corrected for sample heating effects. All spectra have been corrected for the Bose thermal contribution.

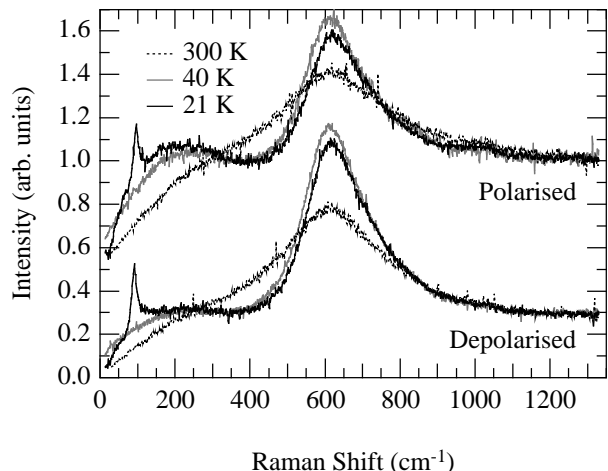


FIG. 1. Polarized (VV) and depolarised (HV) Raman spectra of Crystal A at 300, 40 and 10 K.

Polarised and depolarised Raman spectra of a single crystal of MgB<sub>2</sub> (crystal A) from 15 to 1300  $\text{cm}^{-1}$  are shown in Fig. 1. The spectral intensity has been normalised at high wavenumbers and the polarised spectra offset by 0.5 units along the *y*-axis. Dominating the spectra is a very broad, asymmetric feature located at around

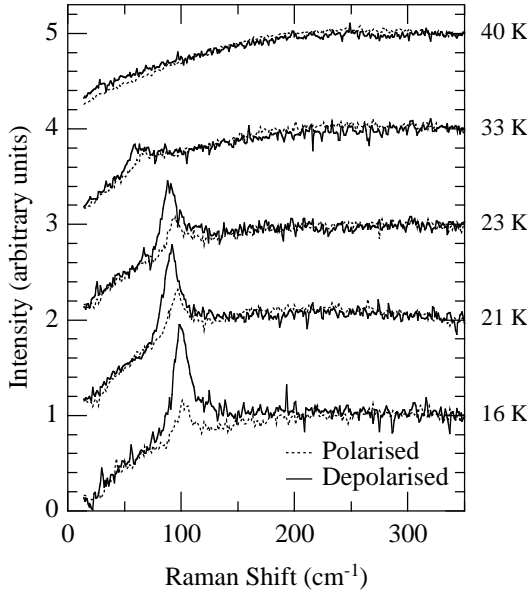


FIG. 2. Polarized and depolarised Raman spectra of crystal A at temperatures  $T \leq T_c$ . Temperatures have been corrected for sample heating effects.

$620\text{ cm}^{-1}$ , which is commonly attributed to the Raman-active  $E_{2g}$  symmetry phonon in  $\text{MgB}_2$  [16]. This feature narrows substantially with decreasing temperature, consistent with calculations which suggest the  $E_{2g}$  phonon is very anharmonic [2], but curiously shows no indication of a large superconductivity-induced hardening below  $T_c$  which might be expected in the presence of strong electron-phonon coupling [1–3]. Cursory modelling of this feature with a Fano equation, an unsatisfactory description of the observed spectral lineshape, revealed  $7\text{--}10\text{ cm}^{-1}$  hardening between 40 K and 21 K. Further measurements must be performed to clarify the character of this mode.

In contrast, a superconductivity-induced renormalization of the electronic continuum is clearly visible in the 21 K spectra, where a sharp pair breaking forms at around  $100\text{ cm}^{-1}$ . Accompanying the peak is a decrease of scattering intensity at lower Raman shifts, although no scattering threshold is seen, and the magnitude of the renormalization is greater in depolarised spectra.

In the case of an isotropic  $s$ -wave gap the theoretically calculated electronic Raman spectrum is characterised by a pair breaking peak located at an energy of  $2\Delta$  in all scattering channels, below which there is zero scattering intensity [12]. For anisotropic  $s$ -wave the scattering threshold remains, located at the minimum gap energy, while pair breaking peaks appear at different Raman shifts in different polarisations, reflecting the gap anisotropy [13,14]. As the polarisation dependence of the peak seen in  $\text{MgB}_2$  is not strongly anisotropic, we associate the pair breaking peak energy with  $2\Delta$  [13,14].

Figure 2 shows Raman spectra from crystal A in the vicinity of the pair breaking peak. The spectra have

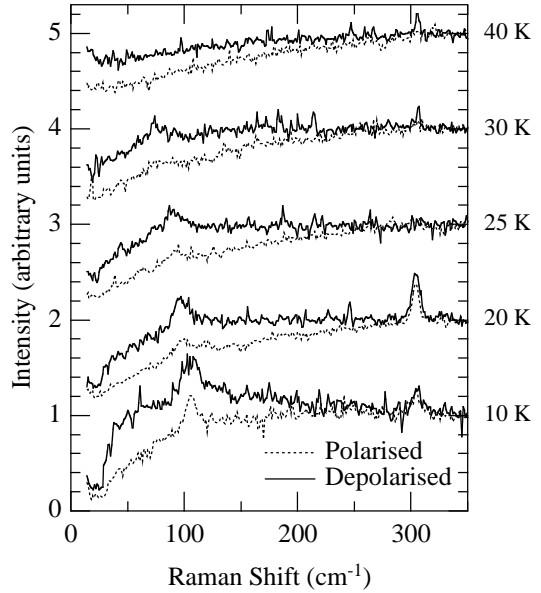


FIG. 3. Polarized and depolarised Raman spectra of crystal B at temperatures  $T \leq T_c$ . The spectra were taken at low laser power and the quoted temperatures are nominal.

been normalized to unity around  $350\text{ cm}^{-1}$  and successive spectra have been progressively offset by one unit along the  $y$ -axis. To obtain an estimate of the gap energy  $2\Delta(T)$ , the spectrum in the vicinity of the pair breaking feature was approximated by a Gaussian with a cubic background, and fitted with a least squares algorithm. Subsequently quoted uncertainties in  $2\Delta(T)$ , are the 95% confidence intervals obtained from the fit.

In Fig. 2 we see the evolution of the  $2\Delta$  peak with temperature and note a small anisotropy in peak energy between polarised and depolarised spectra. The average anisotropy between the two polarisations is  $4 \pm 1\text{ cm}^{-1}$ , the polarised  $2\Delta$  peak always appearing higher in energy than the depolarised peak. A close examination of Fig. 2 suggests that the anisotropy is about  $5\text{ cm}^{-1}$  at temperatures close to  $T_c$ , and falls with decreasing temperature. At the lowest temperatures we were able to measure, the anisotropy is a little less than  $3\text{ cm}^{-1}$ .

It is noteworthy that the continuum below the  $2\Delta$  peak extrapolates linearly to zero intensity in both polarisations and shows neither threshold nor additional structure. The first point suggests that the low-frequency spectrum is electronic in origin, as it exhibits the odd parity expected for electronic Raman scattering.

To verify our results from crystal A we measured the Raman spectrum of a second crystal, crystal B. Low-frequency Raman spectra from crystal B are shown in Fig. 3, where a striking difference between the two crystals is apparent.

While the polarised spectra are comparable between crystals, the depolarised spectra of crystal B show a threshold around  $30\text{--}40\text{ cm}^{-1}$  which is identical to that

seen in polycrystal measurements [17]. We mention here that this crystal showed greater surface contamination and roughness when viewed under a microscope, and shows an impurity feature near  $300\text{ cm}^{-1}$ . The magnitude of the superconductivity-induced renormalization in the depolarised spectra of crystal B is reduced, but  $2\Delta(T)$  is unaffected and agrees well between crystals. Anisotropy of the pair breaking peak position is also present in crystal B, although its average magnitude is slightly smaller than that seen in crystal A, amounting to  $2 \pm 1\text{ cm}^{-1}$ .

In determining superconducting gap symmetry, and thus placing constraints on the underlying mechanism of superconductivity, the temperature dependence of the gap is a convenient test. The BCS theory provides an explicit temperature dependence for a *s*-wave gap with which the experimental data may be compared. We calculate the reduced gap  $2\Delta(T)/2\Delta(0)$  from our data, extrapolating  $2\Delta(0)$  from our lowest temperature measurements. Results of this calculation are shown in Table I.

Sample	Polarisation	$2\Delta(0)$ ( $\text{cm}^{-1}$ )	$2\Delta(0)/k_B T_c$
Crystal A	Polarised	$106 \pm 2$	$3.99 \pm 0.09$
	Depolarised	$103 \pm 1$	$3.88 \pm 0.05$
Crystal B	Polarised	$106 \pm 1$	$4.01 \pm 0.05$
	Depolarised	$105 \pm 1$	$3.96 \pm 0.08$

TABLE I. Extrapolated values of maximum gap energy and the corresponding gap to  $T_c$  ratio.

The magnitude of the superconducting gap energy, averaged between polarisations, is  $2\Delta(0) = 3.96 \pm 0.09$ , which is consistent with  $\text{MgB}_2$  being a moderately strong coupling superconductor.

Figure 4 shows  $2\Delta(T)/2\Delta(0)$  for both crystals, which follow the BCS-predicted temperature dependence. Uncertainties in temperature are shown for those data points of crystal A to which a correction was performed; no correction was made to the crystal B temperatures as low incident laser power was used. The temperature dependence of the superconducting gap, as directly measured by Raman scattering, indicates that  $\text{MgB}_2$  is a conventional phonon-mediated superconductor.

We now turn our attention to the below- $2\Delta$  continuum, which does not display the scattering threshold predicted for a *s*-wave superconductor [12–14]. Raman studies of the  $\text{Nb}_3\text{Sn}$  and  $\text{V}_3\text{Si}$  conventional superconductors [18–20] also show a sharp decrease in scattering intensity below the pair breaking peak, but are somewhat ambiguous regarding the existence of scattering intensity below the gap feature. Recent measurements of nickel borocarbide superconductors show definite scattering intensity below a well-defined  $2\Delta$  peak [21], which led the authors to suggest that this may be an intrinsic aspect of electronic Raman scattering in conventional supercon-

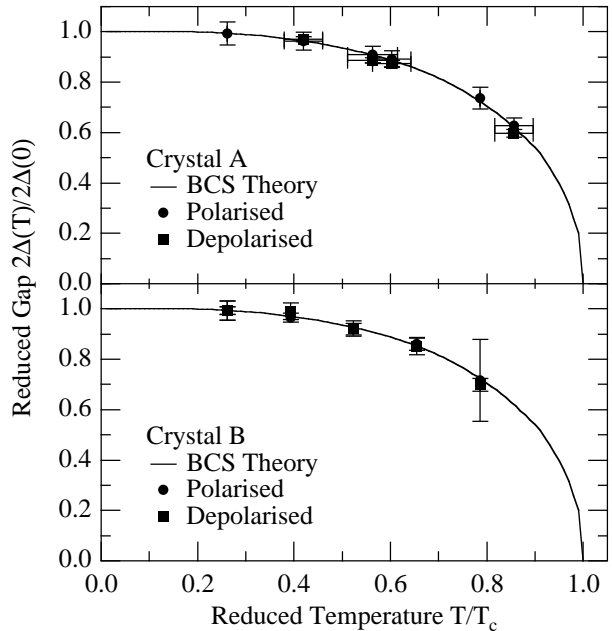


FIG. 4. Reduced gap temperature dependence for crystals A and B. The solid line is the reduced gap from BCS theory.

ductors.

The superconducting-state electronic Raman spectra of crystal A (Fig. 2) have much in common with other conventional superconductors, particularly the nickel borocarbide system, where the  $2\Delta$  peak is similarly sharp but no scattering threshold is seen [21]. We discount the possibility of gap nodes producing the below- $2\Delta$  continuum [13,14]. Contamination is another possible source of low-frequency Raman intensity, and although crystal A was indisputably cleaner than crystal B (cf. Figs. 2 and 3), we are unable to eliminate the possibility of contaminant contribution.

The sharp, slightly anisotropic pair breaking peak seen in  $\text{MgB}_2$  stands in stark contrast to the broadened and very anisotropic pair breaking features observed in *d*-wave high- $T_c$  materials.  $\text{MgB}_2$  is even less anisotropic than some conventional superconductors, for which  $2\Delta$  peak position anisotropies of up to 20% have been reported [18,21]. The difference in the magnitude of the superconductivity-induced renormalization seen in polarised and depolarised spectra are consistent with Raman spectra measured from other superconductors, both conventional and high- $T_c$ . We conclude that our Raman spectra are consistent with the body of Raman results from conventional *s*-wave superconductors and indicative of a slightly anisotropic *s*-wave gap.

We find evidence that crystal B is disordered compared to crystal A, independent of contaminant features. While scattering of quasiparticles by impurities or disorder has only a weak effect on  $T_c$  and  $2\Delta(0)$ , in an anisotropic *s*-wave superconductor they have the effect of reducing

the  $2\Delta$  peak anisotropy [14]. We recall that while  $T_c$  and  $2\Delta(0)$  are identical between crystals, within the quoted uncertainties, the average anisotropy between the two crystals differs by a factor of two. It seems likely that the  $40\text{ cm}^{-1}$  shoulder is not an intrinsic property of MgB<sub>2</sub> related to a second pair breaking peak, rather it appears to be an extrinsic effect related to sample quality.

In summary, we have measured the temperature and polarisation dependence of the  $2\Delta$  pair breaking peak seen in the electronic Raman continuum of MgB<sub>2</sub> single crystals. The temperature dependence of  $2\Delta$  is consistent with a conventional *s*-wave BCS superconducting gap, and the average gap to  $T_c$  ratio  $2\Delta/k_B T_c = 3.96 \pm 0.09$  indicates moderately strong electron phonon coupling. A small anisotropy in the  $2\Delta$  peak position is present in both samples, although slightly smaller in magnitude in our poorer quality crystal. We observe a single gap feature in our Raman spectra, and attribute structure below the pair breaking peak seen in the poorer crystal to contamination. Our Raman measurements reveal MgB<sub>2</sub> to be a conventional BCS superconductor with a slightly anisotropic gap.

This work was supported by the New Energy and Industrial Technology Development Organization (NEDO) as collaborative research and development of fundamental technologies for superconductivity applications.

(2001).

- [3] Y. Kong, O. V. Dolgov, O. Jepsen, O. K. Andersen, Phys. Rev. B **64**, 020501 (2001).
- [4] M. Imada, J. Phys. Soc. Jpn. **70**, 1218 (2001).
- [5] N. Furukawa, J. Phys. Soc. Jpn. **70**, 1483 (2001).
- [6] S. L. Bud'ko, G. Lapertot, C. Petrovic, C. E. Cunningham, N. Anderson and P. C. Canfield, Phys. Rev. Lett. **86**, 1877 (2001).
- [7] T. Takahashi, T. Sato, S. Souma, T. Muranaka and J. Akimitsu, Phys. Rev. Lett. **86**, 4915 (2001).
- [8] G. Rubio-Bollinger, H. Suderow, and S. Vieira, Phys. Rev. Lett. **86**, 5582 (2001).
- [9] H. Schmidt, J. F. Zasadzinski, K. E. Gray and D. G. Hinks, Phys. Rev. B **63**, 220504 (2001).
- [10] A. Sharoni, I. Felner and O. Millo, Phys. Rev. B **63**, 220508 (2001).
- [11] Y. Wang, T. Plackowski and A. Junod, Physica C **355** 179 (2001).
- [12] M. V. Klein and S. B. Dierker, Phys. Rev. B **29**, 4976 (1984).
- [13] T. P. Devereaux and D. Einzel, Phys. Rev. B **51**, 16336 (1995); T. P. Devereaux and D. Einzel, Phys. Rev. B **54**, 15547 (E) (1996).
- [14] T. P. Devereaux, Phys. Rev. Lett. **74**, 4313 (1995).
- [15] S. Lee, H. Mori, T. Masui, Yu. Eltsev, A. Yamamoto and S. Tajima, J. Phys. Soc. Jpn. accepted for publication (2001).
- [16] A. F. Goncharov, V. V. Struzhkin, E. Gregoryanz, J. Hu, R. J. Hemley, H.-k. Mao, G. Lapertot, S. L. Bud'ko and P. C. Canfield, Phys. Rev. B accepted for publication (2001)
- [17] X. K. Chen, M. J. Konstantinović, J. C. Irwin, D. D. Lawrie and J. P. Franck, cond-mat/0104005.
- [18] S. B. Dierker, M. V. Klein, G. W. Webb and Z. Fisk, Phys. Rev. Lett. **50**, 853 (1983).
- [19] R. Hackl, R. Kaiser and S. Shicktanz, J. Phys. C **16**, 1729 (1983).
- [20] R. W. Hackl, R. Kaiser and W. Gläser, Physica C **162–164**, 431 (1989).
- [21] In-Sang Yang, M. V. Klein, S. L. Cooper, P. C. Canfield, B. K. Cho and Sung-Ik Lee, Phys. Rev. B **62**, 1291 (2000).